

Final-State Interactions and the Simulation of Resonances*†

CHRISTOPH SCHMID

California Institute of Technology, Pasadena, California

(Received 25 July 1966)

It is shown that the singularities of the triangle or rescattering diagram cannot produce peaks in the total transition rate. Rescattering bands can be seen on the Dalitz plot, but their projections into invariant-mass plots do not produce peaks, if all events on the Dalitz plot are included. In other words, the Peierls mechanism and its recent variants do not work, even if the singularity is on the physical boundary. The reason is a cancellation of the peak, which occurs when the diagram without rescattering is added coherently to the triangle diagram. It is also shown that interference of overlapping resonance bands does not produce the previously expected peaks in the total transition rate or in the two-body mass plots in three different cases. This result holds to first order in the ratio of the resonance width to the diameter of the Dalitz plot.

I. INTRODUCTION

RESONANCES are observed as peaks in invariant-mass plots, but are all the peaks really resonances? Can some of the peaks be explained as kinematical effects? Can we find mechanisms which produce peaks without resonances?

We shall discuss two groups of effects, which have been assumed to be capable of simulating resonances. Both arise from final-state interactions of three particles. We shall show that neither can produce peaks.

The first group of effects is based on the singularities of the triangle or rescattering diagram. These are the different versions of the Peierls¹ mechanism for generating three-body peaks. Goebel and others² have pointed out that the original version does not work, because the singularity lies on the wrong Riemann sheet. However, in the modified and inverted versions³ the singularity can be on the correct sheet, i.e., on the physical boundary. There has been criticism that these peaks would be small and unimportant. What we shall prove is that they do not exist at all: The singularity on the physical boundary will not produce a peak in the total transition rate or in the mass plots, because one must add another diagram (primary production without rescattering), and the peak disappears in the process of coherent addition. On the other hand, the singularity does produce a weak rescattering band on the Dalitz plot, but its projection into the invariant-mass plot does not show a peak, if we include all events on the Dalitz plot.

The second group of suspected peaking effects has to do with interference of overlapping resonance bands.⁴ We shall show again that they produce no peaks in the total transition rate or in the invariant-mass plots.

* Work supported in part by the U. S. Atomic Energy Commission. Prepared under Contract No. AT(11-1)-68 for the San Francisco Operations Office, U. S. Atomic Energy Commission.

† Based on parts of the Ph.D. thesis submitted to the Physics Department of the Massachusetts Institute of Technology, February 1966.

¹ R. F. Peierls, Phys. Rev. Letters **6**, 641 (1961).

² C. Goebel, University of Wisconsin Report, 1962 (unpublished); Phys. Rev. Letters **13**, 143 (1964); R. C. Hwa, Phys. Rev. **130**, 2580 (1963); P. K. Srivastava, *ibid.* **131**, 461 (1963); I. J. R. Aitchison and C. Kacsar, *ibid.* **133**, B1239 (1964).

³ See, e.g., C. Kacsar, Phys. Letters **12**, 269 (1964).

⁴ See, e.g., J. Gillespie, *Final-State Interactions* (Holden-Day, Inc., San Francisco, California, 1964).

Section II deals with the first group of effects, the different versions of the Peierls mechanism. They are reviewed in part A. There we discuss those aspects, mainly kinematical, which can be understood without a detailed knowledge of the triangle diagram. The important tool is the theorem of Coleman and Norton,^{5,6} with its classical space-time picture. In part B, we state our fundamental equation (12), interpret it in physical terms, and arrive at our conclusions about the observable effects of the triangle diagram and the absence of peaks in transition rates and invariant-mass plots. In part C, we prove the fundamental equation, first in perturbation theory, and then in the dispersion theory of final-state interactions. Parts D and E should be skipped by the general reader who is only interested in the absence of peaks in the mass plots, but not interested in the calculation of the weak rescattering band. In part D, we give the kinematics and the analytic properties of the Born amplitude in order to fill in details for part C and to prepare and introduce notation for part E, where we shall derive a convenient, explicit expression for the triangle amplitude.

Section III treats the second group of effects, three effects based on the interference of overlapping resonance bands. First we shall explain why peaks were expected, and afterwards we shall show why such peaks do not arise.

II. TRIANGLE SINGULARITIES, RESCATTERING EFFECTS, AND THE PEIERLS MECHANISM

A. The Different Mechanisms and the Triangle Singularities

1. The Original Version of the Peierls Mechanism

Peierls¹ considered the diagram of Fig. 1 and observed that this one-particle exchange pole can be inside the

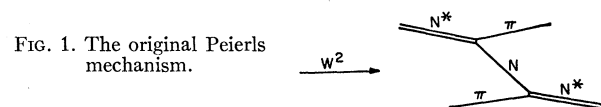


FIG. 1. The original Peierls mechanism.

⁵ The general theorem was given by S. Coleman and R. E. Norton, Nuovo Cimento **38**, 438 (1965).

⁶ The theorem in the special case of the triangle amplitude was first given by J. B. Bronzan, Phys. Rev. **134**, B687 (1964).

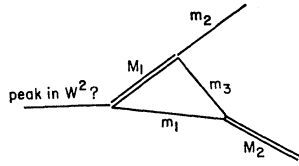


FIG. 2. The triangle diagram for the original Peierls mechanism, $M_1 = M_2 = N^*$ (1238), $m_1 = m_2 = \pi$, $m_3 = N$. M_2 is fixed, the singularity in W^2 is on the wrong sheet.

physical region, i.e., the physical scattering amplitude can become (almost) infinite. Because the exchanged nucleon can be on the mass shell, it can travel infinitely far before it is reabsorbed, and this produces an infinite range of interaction.

Experimentally, we cannot have a beam of incident N^* . Therefore we study the production process $N + \pi \rightarrow N + \pi + \pi$. The Peierls diagram enters by unitarity: The N^* is produced by some primary interaction, and the three-body interaction, i.e., the final-state interaction, is represented by the Peierls diagram. Because we are only interested in the structure caused by the final-state interactions, and because we know nothing about the structure of the primary production vertex, we replace it by a point vertex and arrive at the triangle diagram of Fig. 2. W is the invariant mass in the initial two-body channel $N + \pi$.

Naive unitarity seems to suggest that the peaks in the amplitude of the Peierls diagram (Fig. 1) would produce peaks in the (imaginary part of the) whole amplitude (Fig. 2). This argument is wrong, because the generalized unitarity relation gives the discontinuity and not the imaginary part (see part C of this section). If it were right, as originally supposed by Peierls, a peak in W^2 would simulate a three-body resonance in the final state. The predicted energy is 1490 MeV, suggestively close to the N_{1518}^* ($\frac{1}{2}^-, \frac{3}{2}^-$). Peierls¹ also predicted four other N^* peaks, and others⁷ applied the mechanism to meson and hyperon systems. Everywhere one obtained a lot of predictions for peaks, and the agreement with the measured energies seemed to be good, although there are no free parameters in the predicted energies. It is usually not possible, however, to assign definite quantum numbers, because kinematical peaks show up in several angular momentum and isospin channels. Only under special circumstances will a peak be much stronger in one particular channel.^{1,7}

This is the Peierls mechanism in the original version where the initial and final states (in Fig. 1) are the same. This version does not work, because the singularity is on the wrong Riemann sheet, as shown by Goebel.² Let us

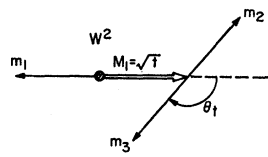


FIG. 3. Classical space-time process discussed in connection with the triangle diagram.

⁷ M. Nauenberg and A. Pais, Phys. Rev. Letters 8, 82 (1962); R. J. Oakes, *ibid.* 12, 134 (1964); S. F. Tuan, Phys. Rev. 125, 1761 (1962).

now find out where the triangle singularities are located, at what energies, and on which sheets. We consider the generalized case,³ where all masses are different.

2. Location of the Triangle Singularities

The two triangle singularities appear at the highest and lowest energy W^2 which allows all three internal lines of Fig. 2 to be on their respective mass shells simultaneously. This is the same as putting all lines on their mass shells and the rescattering angle (= scattering angle of Fig. 1) at its two extreme values $z = \pm 1$. Then all vectors are parallel in the center-of-mass frame.

What do we mean by "wrong sheet"? The triangle amplitude has a threshold singularity at $W^2 = (M_1 + m_1)^2$. This is where the right-hand branch cut (unitarity cut) starts, and the physical region (= physical boundary) is just above the cut. If we move upwards, we never find any singularity. If we move downwards, the cut is in our way and forces us to go into the second sheet immediately. If we find a singularity here, it is very close to the physical region. On the other hand, if a singularity lies above the axis on the second sheet or below the axis on the first sheet,⁸ it is far away from the physical region.

On which sheet are the triangle singularities? Coleman and Norton⁵ and others⁶ gave a simple and general answer. The singularity of a Feynman amplitude is on the physical boundary if, and only if, the diagram can be interpreted as a classical process in space-time. For the rescattering process (triangle amplitude), this means (see Fig. 3): All three internal particles must be on their mass shells, the decaying M_1 must emit the m_3 in the backward direction ($\theta_i = \pi$), m_3 must have enough speed to catch up with m_1 in order to rescatter, and m_1 and m_3 must have enough relative velocity to form M_2 . The condition of Coleman and Norton also implies that the singularity which corresponds to $\theta_i = 0$ is never on the physical boundary.

Let us determine the energies of the singularities. We assume that W^2 is given and ask what the mass M_2 is which is being formed. We start with the minimum value $W_{\min}^2 = (M_1 + m_1)^2$. Then M_1 and m_1 are created at relative rest. The invariant mass of m_1 and m_3 will be called s , and it is given by

$$s_{\max} = m_1^2 + m_3^2 + 2m_1 E_3, \quad (1)$$

$$E_3 = (M_1^2 + m_3^2 - m_2^2)(2M_1)^{-1}. \quad (2)$$

We call this s value s_{\max} , because s will decrease upon an increase in W^2 . M_1 and m_1 will move apart with increasing velocity, and it will become harder for m_3 to catch up with m_1 . The invariant mass s decreases to the point where m_1 and m_3 have zero relative velocity and $s = s_{\min} = (m_1 + m_3)^2$. The corresponding value of W^2 is called W_{\max}^2 and it is easily determined in the rest

⁸ Such a singularity is on the first sheet with respect to the threshold $W^2 = (M_1 + m_1)^2$, but on the second sheet with respect to the threshold $W^2 = (m_1 + m_2 + m_3)^2$, which is far away and neglected in our treatment.

system of m_1 and m_3 :

$$W_{\max}^2 = M_1^2 + m_1^2 + 2m_1 E_1, \quad (3)$$

$$E_1 \equiv E(M_1) = (M_1^2 + m_3^2 - m_2^2)(2m_3)^{-1}. \quad (4)$$

E_1 is the energy of the decaying particle M_1 viewed from the rest frame of the decay product m_3 .

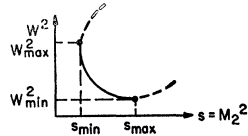
The results of this analysis are contained in Fig. 4, where the minimum values are the respective thresholds and the maximum values are given by Eqs. (1) to (4). The dashed line for $s > s_{\max}$ corresponds to the particle m_3 moving in the wrong direction, the dashed line for $W^2 > W_{\max}^2$ to the particle m_3 not having enough velocity to catch up.

The original Peierls mechanism ($M_1 = M_2$) gives singularities in W^2 on the wrong sheet, because M_2^2 is larger than s_{\max} , i.e., Fig. 2 cannot be interpreted as a classical process.

3. The Modified Peierls Mechanism

Here⁹ one takes two different resonances, M_1 high above the threshold $m_2 + m_3$, and M_2 low with respect to the threshold $m_1 + m_3$; i.e., for a given M_1 , one chooses M_2 below the value $\sqrt{s_{\max}}$ of Eq. (1) and Fig. 4. This

FIG. 4. The triangle singularity in W^2 as a function of s and vice versa. Full line: The singularity is on the physical boundary.



choice makes the rescattering process classically possible, and the lower one of the two triangle singularities will lie on the physical boundary.

It turns out that the interval $s_{\min} \leq M_2^2 \leq s_{\max}$ is quite narrow in most cases, particularly for three-meson systems. This makes it difficult to find physical examples.

An example is the $K\bar{K}\pi$ system shown in Fig. 5, with $M_1 = K^*(891)$ and $M_2 = K\bar{K}(1025, I=1)$.¹⁰ Although M_1 is fairly high above the threshold $(K+\pi) = 630$ MeV, $\sqrt{s_{\max}}$ is only 1030 MeV, which is close to the threshold $(K+\bar{K}) = 990$ MeV, and M_2 must lie in this narrow interval (990, 1030). Figure 4 tells us that because the experimental value $M_2 = 1025$ MeV is near the upper end of this narrow interval, W will be very close to $W_{\min} = (K^* + \bar{K}) = 1385$ MeV. It was suggested that this singularity in W could produce the $K\bar{K}\pi$ peak¹¹ at 1420 MeV, named the E meson.

Another example, discussed by Aitchison,¹² is the $N\pi\pi$ system with $M_1 = \rho$, $M_2 = N^*(1238)$. He thought this

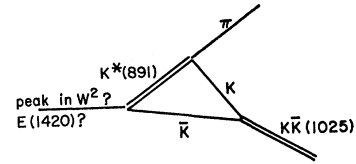
⁹ Kacser (Ref. 3) uses (as we do) the term "generalized Peierls mechanism" for $M_1 \neq M_2$. He then distinguishes between the two possibilities that (i) the singularities are on the wrong sheet as in the original version, or (ii) one of the singularities is on the correct sheet. For this second possibility, we use the term "modified Peierls mechanism."

¹⁰ R. Armenteros *et al.*, Phys. Letters **17**, 344 (1965).

¹¹ P. Baillon *et al.*, CERN Report, 1966 (unpublished).

¹² I. J. R. Aitchison, Phys. Rev. **133**, B1257 (1964).

FIG. 5. The modified Peierls mechanism ($M_1 \neq M_2$, M_2 close to threshold): M_2 is fixed, the singularity in W^2 is on the correct sheet, but we shall find no peak.



might possibly account for the $N^*(1688)$. Kacser³ considered the $\Xi K\pi$ system with $M_1 = K^*$ and $M_2 = \Xi^*(1533)$, but concluded that the effect would be rather too small to be observable at present.

A related possibility is shown in Fig. 6: One works without the resonance M_2 and keeps s fixed experimentally (at a low value). According to Kacser³ this should be called triangle mechanism rather than Peierls mechanism. Such peaks in W^2 have been calculated by Aitchison¹² for the $N\pi\pi$ system with $M_1 = N^*$ and rescattering between the two π 's (Fig. 6). It has been suggested by Kacser and Aitchison¹³ that such peaks could be studied more easily in nuclear physics where the statistics are better. They considered, e.g., the $\alpha\alpha p$ system with $M_1 = \text{Li}^{5*}$ (16.81 MeV) and rescattering between the two α particles, and they made calculations suggesting that 25% effects would occur.

4. The Inverted Peierls Mechanism

In the modified Peierls mechanism, s is fixed at M_2^2 and one looks for a peak in W^2 ; in the inverted Peierls mechanism, one fixes W^2 (by taking a weak or strong decay or an experiment at fixed beam energy) and looks for a peak in s , which might simulate a two-body resonance. One assumes as input a nonresonant rescattering of the particles m_1 and m_3 (point vertex or scattering length approximation). Of course, in both mechanisms the peak is supposed to occur at that W^2 or s where the triangle singularity lies on the physical boundary.

An example is the study of the di-pion in the $\text{He}^3\pi\pi$ final state at low energies. This is where the ABC resonance was discovered,¹⁴ and Anisovich and Dakhno¹⁵ used the triangle diagram (Fig. 7) to explain the ex-

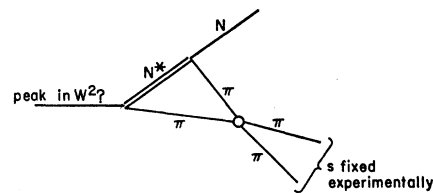


FIG. 6. The modified Peierls mechanism with s fixed experimentally at a low value: The singularity in W^2 is on the correct sheet, but we shall find no peak.

¹³ C. Kacser and I. J. R. Aitchison, Rev. Mod. Phys. **37**, 350 (1965).

¹⁴ N. E. Booth, A. Abashian, and K. M. Crowe, Phys. Rev. Letters **7**, 35 (1961).

¹⁵ V. V. Anisovich and L. G. Dakhno, Phys. Letters **10**, 221 (1964); Zh. Eksperim. i Teor. Fiz. **46**, 1152 (1964) [English transl.: Soviet Phys.—JETP **19**, 779 (1964)].

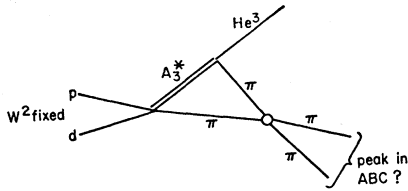


FIG. 7. The inverted Peierls mechanism: W^2 is fixed at a low value, the singularity in s is on the correct sheet, but we shall find no peak. A_3^* = excited state of baryon number 3.

perimental $\pi\pi$ peak without assuming any structure in the $\pi\pi$ interaction.

Analogous effects have been calculated for the di-pion in the $N\pi\pi$ final state with $M_1=N^*(1238)$ in Refs. 12 and 15 and have been compared with experiment in Ref. 15. Striking peaks were computed by Chang and Tuan¹⁶ for the $K\pi$ in the $\Xi K\pi$ final state with $M_1=\Xi^*(1530)$. On the other hand, Bronzan⁶ studied the $NN\pi$ final state with $M_1=N^*(1238)$ numerically and did not get an observable peak. Peaks in nuclear physics experiments are discussed in Ref. 13 using a variation of Fig. 6 where one fixes W^2 and looks for a peak in s .

Because the inverted mechanism assumes no M_2 resonance, one must take two rescattering diagrams instead of one: Both decay products of M_1 may rescatter with m_1 , at least if W^2 is fixed at a low value. For high W^2 none of the two decay products is able to catch up with m_1 ; for intermediate values of W^2 , only the lighter one. We shall keep this in mind, but discuss explicitly only one of the two analogous diagrams.

5. The Weak Peierls Mechanism

The original Peierls mechanism produced singularities on the wrong sheet, but it predicted many of the resonances and the predicted energies were suggestive. The modified mechanism produces singularities close to the physical boundary, but it is difficult to find examples where M_1 is high enough and M_2 low enough.

It was suggested by Low¹⁷ that one could do without an M_2 resonance, but instead take a large scattering length for the rescattering. This corresponds to a nearby pole (bound state or virtual state), whose existence must first be established. This is again essentially the modified mechanism with the difference that the pole M_2 is now below threshold.

On the other hand, Month¹⁸ proposed that one does not need any M_2 pole as input in the s channel in order to produce a peak in W^2 . He argues that a resonance M_2 ,

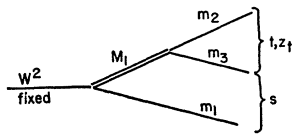


FIG. 8. The resonance-production graph.

¹⁶ Y. F. Chang and S. F. Tuan, Phys. Rev. **136**, B741 (1964).

¹⁷ F. E. Low (unpublished).

¹⁸ M. Month, Phys. Letters **18**, 357 (1965).

whatever its mass, can produce a peak only in the narrow interval (W_{\min}^2, W_{\max}^2) . If one assumes no structure in the s channel and lets M_2 vary over all energies, one averages over the peaks in the narrow interval and this might produce a peak again. The first objection is that the inverted argument would hold as well, and one could now produce a peak in both variables, W^2 and s , with only M_1 as input, while before one needed a pole in one variable in order to produce a logarithmic singularity in the other variable. The second objection concerns the type of singularity produced: In the modified Peierls mechanism, a pole in s produces the triangle singularity in W , which is of the type $(\ln W)$, i.e., it is infinite. In Month's proposal, on the other hand, one must integrate the transition rate over s , and the end point of the integration at s_{\min} = threshold produces a singularity in W at W_{\max} on the physical boundary. But this singularity now is of the type $(W \ln W)$ and therefore finite.

6. The Formula for the Triangle Singularities

Let us now turn to some mathematical detail and calculate the singular energies. Consider first the modified Peierls mechanism where s is fixed at M_2^2 , and put all particles on their mass shell. W is the invariant mass of M_1 and m_1 , and the energies and momenta of both particles are easily calculated in the rest frame of m_3 :

$$E(M_1) = (M_1^2 + m_3^2 - m_2^2) / 2m_3, \tag{5}$$

$$p(M_1) = (1/2m_3) [M_1^2 - (m_2 + m_3)^2]^{1/2} \times [M_1^2 - (m_2 - m_3)^2]^{1/2}, \tag{6}$$

$$E(m_1) = (M_2^2 - m_1^2 - m_3^2) / 2m_3, \tag{7}$$

$$p(m_1) = (1/2m_3) [M_2^2 - (m_1 + m_3)^2]^{1/2} \times [M_2^2 - (m_1 - m_3)^2]^{1/2}, \tag{8}$$

$$W^2 = M_1^2 + m_1^2 + 2E(M_1)E(m_1) (\pm) 2p(M_1)p(m_1). \tag{9}$$

One sees from Fig. 4 and from the space-time picture that one must choose the lower root.

An analogous formula holds for the inverted mechanism. The explicit formula (9), with (5) to (8) inserted, is quite complicated, but fortunately it is needed only for exact numerical calculations. For a qualitative discussion one can more easily use the space-time picture or follow the singularities on the Mandelstam-Dalitz plot. (See the end of the next section.)

7. Classical Rescattering on the Dalitz Plot

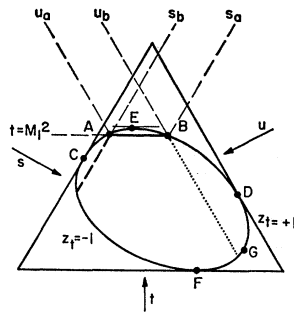
In order to become familiar with the patterns on the Dalitz plot, we first study the classical case, where all internal particles are on the mass shell and travel a long distance between successive interactions at the vertices. Besides the invariants s, t , and u , it is helpful to also use the pair of variables (t, z_t) , where z_t is the cosine of the decay angle θ_t of the resonance at $t = M_1^2$, measured in the rest frame of M_1 (Fig. 3). We convince ourselves

that s is linear in z_t (for fixed t) by calculating s in the rest frame of M_1 . Therefore, $z_t = \pm 1$ is on the boundary of the Dalitz plot and this corresponds to collinear events, i.e., all vectors are parallel in the overall rest frame.

If we have resonance production without rescattering (Fig. 8), we know that the event must lie somewhere on the band $t = M_1^2$ in Fig. 9. Exactly where it lies depends on the decay angle: If θ_t is π , then m_2 moves forward (Fig. 3), its kinetic energy T_2 assumes its maximum, the invariant mass s of m_1 and m_3 assumes its minimum (for t fixed at M_1^2), and the event lies at the point A.

Now we turn to rescattering: m_3 moves backward, and if it can catch up with m_1 , these two particles will rescatter elastically. Their invariant-mass s will stay unchanged and the event on the Dalitz plot will be displaced along the dashed line. It will be displaced *downward* along the dashed rescattering band, because rescattering increases the kinetic energy of m_1 and decreases the invariant mass t of m_2 and m_3 . Moving events downward is possible only if the point A is above the point C. At C, s assumes its minimum value, m_1 and m_3

FIG. 9. Rescattering in the $K\bar{K}\pi$ system: $M_1 = K^*$, $m_1 = \bar{K}$, $m_2 = \pi$, $m_3 = K$.



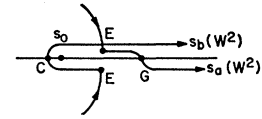
are at relative rest, and m_3 just barely manages to catch up with m_1 . If A is below C, rescattering is impossible.

At the point B, it is the particle m_2 which moves backwards and can catch up with m_1 if its velocity is high enough, i.e., if B is above D. Rescattering displaces the event downwards on the plot along the dotted line of constant u .

From this Dalitz plot we can read off the motion of the singularities (of the triangle amplitude) in the s plane under a variation of W^2 (see Fig. 10). We have seen that the singularity s_b (i.e., the rescattering band) appears at the point where the resonance band leaves the Dalitz plot. At the other end of the resonance band $s = s_a$ and rescattering between m_1 and m_3 is never possible. Therefore, the singularity s_a must always be on the wrong sheet.

When $W^2 = (M_1 + m_1)^2$, the resonance band touches the Dalitz plot at E, and the two singularities s_a and s_b coincide (apart from the small imaginary parts). Upon increasing W^2 they move apart until s_b reaches its threshold value s_0 at C. After that, s_a and s_b both increase (Fig. 10). Note that it is only the short piece

FIG. 10. The triangle singularities in the s plane as functions of the real parameter W^2 .



between C and E (in Figs. 9 and 10) which represents a singularity on the correct sheet.

Are s_a and s_b above or below the real axis? We have seen that they occur where the resonance band $t = M^2 - iM\Gamma$ crosses the boundary of the Dalitz plot. Between C and E and between F and G, we find that $(\partial s / \partial t)$ is positive along the boundary, so the singularity in s is below the axis. Vice versa for the boundary between E and G and between C and F.

B. Effects of the Triangle Singularities: The Fundamental Equation

The modified and the inverted Peierls mechanisms do not produce peaks, even if the singularity is just below the physical boundary.

In order to prove our statement, we observe that along with the triangle amplitude $A^{(t)}$ of Fig. 11(a) we should also consider the resonance production (or primary interaction) amplitude $A^{(r)}$ of Fig. 11(b). The triangle amplitude $A^{(t)}$ represents a rescattering correction to the resonance production amplitude $A^{(r)}$, and both must be added together coherently. Convenient variables for this purpose are s and z_s , the cosine of the "decay" angle of the s system in its own rest frame, i.e., the angle between m_1 and m_2 in the rest frame of s . The invariant mass distribution $R(s)$ is the sum of the distributions in the partial waves,

$$R(s) = r \sum_{l=0}^{\infty} (2l+1) |A_l(s)|^2, \quad (10)$$

where r is the width of the Dalitz plot at a given s . The different partial waves add incoherently because the Legendre polynomials $P_l(z_s)$ are an orthogonal system on the Dalitz plot (for every fixed s). The partial-wave amplitude A_l is the sum of the triangle amplitude $A_l^{(t)}$ and the resonance production amplitude $A_l^{(r)}$,

$$A_l(s) = A_l^{(r)}(s) + A_l^{(t)}(s). \quad (11)$$

The crucial observation is that $A_l^{(r)}$ cannot be considered as a background term because it also has singularities, indeed singularities of exactly the same form and at exactly the same energy as $A_l^{(t)}$. The only

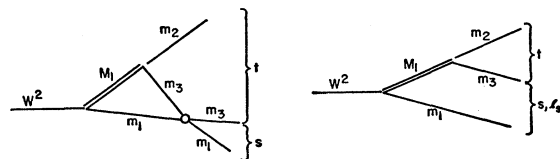


FIG. 11. (a) The triangle amplitude $A^{(t)}$ (rescattering amplitude). No structure assumed for the elastic (m_1, m_3) amplitude. (b) The resonance production amplitude $A^{(r)}$.

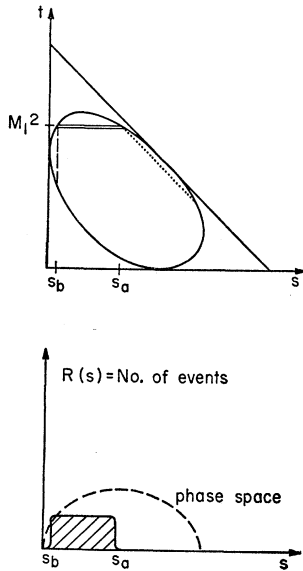


FIG. 12. (a) Dalitz plot for the Feynman diagrams shown in Figs. 11(a) and 11(b). (b) The corresponding invariant-mass distribution.

difference is that $A_i^{(r)}$ has both singularities s_a and s_b on the physical boundary, while $A_i^{(t)}$ has the one with the higher energy, s_a , on another Riemann sheet.

If we denote the singular part of a function A by \tilde{A} , the *fundamental result*, which shall be proved in part C of this section, is

$$\tilde{A}_i^{(r)} + \tilde{A}_i^{(t)} = S_i \tilde{A}_i^{(r)} \quad \text{for } s \simeq s_b, \quad (12)$$

where S_i is the elastic (m_1, m_3) scattering matrix, and s_b is the lower of the two singular points of $A_i^{(r)}$. The effect of the rescattering diagram is therefore nothing more than a multiplication of the singularity from the resonance-production diagram by a phase factor S_i .

Let us describe what happens on the Dalitz plot in Fig. 12(a) (for fixed W^2). The resonance production diagram $A^{(r)}$ of Fig. 11(b) produces by means of its pole the usual resonance band at $t = M_1^2$. The corresponding invariant-mass distribution in s (a projection of the Dalitz plot) is shown in Fig. 12(b) and, as we expect, it is a step function with singularities at s_a and s_b . The partial-wave contributions behave like $|\ln(s - s_a)|^2$ near s_a , like $|\ln(s - s_b)|^2$ near s_b and are peaked at s_a and s_b for low partial waves.

The rescattering diagram (triangle diagram) has a logarithmic singularity at $s = s_b$, which produces the rescattering band in Fig. 12(a) (vertical, dashed band). One might think that its projection into the invariant-mass plot would produce a peak. That this is not the case can be seen from Eqs. (10) and (12): The inclusion of the triangle diagram does not change the invariant mass plot at s_b , therefore the inverted Peierls mechanism does not work.

$|A^{(r)}|^2$ produces the horizontal band, the interference term $2\text{Re}(A^{(r)}A^{(t)*})$ removes events from the overlap region with the vertical band, and $|A^{(t)}|^2$ puts the same number of events back on the Dalitz plot in the form of a weak vertical band.

In the modified Peierls mechanism we have resonant rescattering, i.e., the triangle amplitude is multiplied by a resonance factor with peak at $s = M_2^2$. To get the total transition rate, we have to integrate over the invariant-mass plot. The triangle diagram (with resonant rescattering) by itself has two peaks: the rescattering peak at $s = s_b$ and the resonance peak at $s = M_2^2$. For one particular total energy $W = W_b$, the two peaks coincide and one would expect a peak in the total transition rate. However, if we take the sum of the two diagrams $A^{(t)}$ and $A^{(r)}$, both peaks are absent in the invariant-mass plot. Therefore, no special effect occurs for $W = W_b$ when the two singularities coincide, and the modified Peierls mechanism also does not work.

We conclude that the singular part of the rescattering amplitude [Fig. 11(a)] has exactly the effects that are expected classically:

(1) It does not change the total number of events on the Dalitz plot, i.e., the total transition rate is not enhanced at the singular energy (no modified Peierls mechanism).

(2) It shifts the events on the Dalitz plot around in a very special way: The invariant mass of the rescattered particles stays unchanged. Therefore, there will be no peak in the projection of the Dalitz plot (no inverted Peierls mechanism).

(3) It produces a weak rescattering band on the Dalitz plot; however, as stated under (2), the projection of this band does not give a peak if we project the entire Dalitz plot, since the same number of events is missing from the overlap region. This rescattering band is an observable effect of the triangle diagram, and it has been detected in nuclear physics by J. Lang *et al.*¹⁹ Their three-body system is C^{12}, p, n ; $M_1 = N^{13*}$ (3.56 MeV) and the rescattered pair is (p, n) . The effect is barely observable, and the peak is about 100 times smaller than the true N^{13*} resonance peak and about four times smaller than the background. Theory and experiment are in rough agreement.²⁰

It is not surprising that we arrive at these classical results when we consider the singular part of Feynman diagrams, because singularities arise when all particles are on their mass shells and can travel infinitely far between successive interactions.

The situation is basically different, if a stable particle such as the deuteron appears in the final state as the particle M_2 , because the diagram $A^{(r)}$ is absent (if the deuteron is detected), or it is not added coherently (if the deuteron is not detected). If the deuteron appears in initial and final states, then one needs a separate discussion.

Let us now discuss two objections to the conclusion that no peaks will be produced in the total transition rates and in the invariant-mass plots.

¹⁹ J. Lang *et al.*, Phys. Letters 15, 248 (1965).

²⁰ J. Lang *et al.*, Nucl. Phys 88, 576 (1966).

(a) We have not discussed the regular part of the triangle amplitude. It cannot be neglected, particularly since the logarithmic singularity is a weak one. It is well possible that this regular part shows bumps. However, there is no reason why such a bump should appear close to the triangle singularity s_b .

(b) It has been suggested that the interference term between the singular part of $A^{(t)}$ and some background (or the regular parts of $A^{(t)}$ and $A^{(r)}$) would give an effect. However, exactly the same small effect will also be produced without even including the rescattering diagram: interference between the singular part of $A^{(r)}$ and, e.g., some smooth s -wave background. Such effects modify the step function of Fig. 12(b) a little bit, by superimposing a weak peak or dip, but they have nothing to do with rescattering.

We have discussed a final-state interaction which cannot produce peaks. On the other hand, the most basic final-state interaction gives very important peaks, the resonances themselves. In our framework, this interaction is described by the Feynman diagram, Fig. 11(b), which produces a peak in the (m_2, m_3) system and is not a rescattering effect, but rather a two-body decay into M_1 and m_1 . The theorem of Coleman and Norton and the corresponding picture of a classical rescattering process does not make statements about Fig. 11(b). In this sense, it is still true that rescattering effects do not enhance.

But in another sense, rescattering effects do enhance: Figure 11(b) represents the sum over infinitely many complicated rescattering diagrams, each of which fails to produce a singularity in the physical region. But the sum is singular, and the singularity is the M_1 -resonance pole.

This resonance pole is a truly dynamical effect, and the corresponding peak can be calculated neither by perturbation theory nor by a dispersion theory of final-state interactions.⁴ What can be calculated in these two theories is the manifestation of one resonance pole in different final states, e.g., the manifestation of the N^* in the photoproduction of a π . The fact that truly dynamical effects are not calculated, but are a phenomenological input, is implied by the resonance propagator in Fig. 11(b).

A similar reasoning applies to the question of whether multiple rescattering graphs [Fig. 16(c)] can change our conclusions. One such graph by itself will always be regular on the physical boundary, because it cannot be interpreted as a classical process. But can these graphs sum to a singularity, e.g., to a three-body resonance pole? This is possible; but again, this would be a truly dynamical effect and could not be calculated in the usual dispersion theory of final-state interactions. On the other hand, Hwa² discussed such dynamical effects, and he suggested that the triangle singularities which are on the wrong sheet might induce a true resonance pole on the correct sheet at a *nearby* energy. In this

case, the triangle singularity would work as a kind of force. Gyuk and Tuan²¹ came to the conclusion that this works for baryonic three-body systems, while Tuan²² found that it does not work for mesonic systems. Such effects are truly dynamical effects (the induced singularities are not given by algebraic formulas), while the effects discussed in this paper are kinematical ones (the triangle singularities are given by an algebraic formula). Another distinction is that Hwa tries to *generate* (true) resonances, while we have discussed attempts to *simulate* resonances. Thus our discussion does not bear upon Hwa's proposal. Other dynamical calculations have been performed in the Lee model and the static model.²³

C. Proof of the Fundamental Equation

The fundamental equation (12) will first be derived for the lowest order perturbation graph (the triangle graph), where the rescattering vertex is replaced by a point. This Feynman graph contains an unstable internal line, but Aitchison and Kacser²⁴ have shown that such a diagram has a well-defined meaning. It is treated by replacing Feynman's $i\epsilon$ in the corresponding denominator by $iM\Gamma$, which removes an eventual singularity from the physical boundary by a small distance.

There are two methods to discuss and evaluate a Feynman amplitude: One is to introduce Feynman parameters and to integrate the internal momenta first. The other one is to use Cutkosky's rule²⁵ and to write the amplitude as a dispersion integral. (This is a mathematical trick within the framework of perturbation theory and must be distinguished from dispersion theory.) In both methods it is not possible to perform the last integration using the commonly known functions of mathematical physics.²⁶ However, the second method has several advantages: The integrand has a direct physical meaning. It allows a recursive discussion of singularities: The leading singularities of a complicated diagram are the singularities of a simpler diagram. Dispersion integrals also exhibit explicitly singularities and the complete sheet structure. Finally they lend themselves easily to approximation methods.

We shall concentrate on the inverted mechanism and derive the dispersion representation in s for fixed W^2 . (This is equivalent to the dispersion representation in W^2 for fixed s , because both are derived from the same Feynman integral.)

²¹ I. P. Gyuk and S. F. Tuan, *Nuovo Cimento* **32**, 227 (1964).

²² S. F. Tuan, *Phys. Letters* **11**, 248 (1964).

²³ R. F. Peierls and J. Tarski, *Phys. Rev.* **129**, 981 (1963); B. d'Espagnat and F. M. Renard, *Nuovo Cimento* **30**, 536 (1963); T. L. Trueman, *Phys. Rev.* **137**, B1566 (1965); I. J. R. Aitchison, *Nuovo Cimento* **34**, 508 (1964); P. K. Srivastava, *Phys. Rev.* **131**, 461 (1963).

²⁴ I. J. R. Aitchison and C. Kacser, *Phys. Rev.* **133**, B1239 (1964).

²⁵ R. E. Cutkosky, *J. Math. Phys.* **1**, 429 (1960).

²⁶ A. C. T. Wu, *Kgl. Danske Videnskab. Selskab, Mat. Fys. Medd.* **33**, No. 3 (1961) has shown how to express the triangle amplitude in terms of Spence functions.

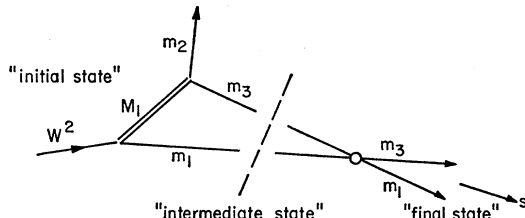


FIG. 13. Cutkosky's rule.

The threshold singularity $s_0 = (m_1 + m_3)^2$ appears at the lowest s value which allows the internal m_1 and m_3 to be on their mass shells simultaneously. Other normal thresholds, e.g., $W^2 = (M_1 + m_1)^2$, do not appear since the two external lines W and m_2 are kept at fixed masses. The pseudothreshold in s at $(m_1 - m_3)^2$ is not a singularity on the first sheet, because it is the highest value at which particles m_1 and m_3 can be on their mass shells, with one of them going backwards in time. Also, the external thresholds $s = (W \pm m_2)^2$ are not singularities on the first sheet for our amplitudes. The only other singularities which have a chance of being on the first sheet are the triangle singularities. They are most easily discussed by first determining the discontinuity across the threshold cut starting at $s_0 = (m_1 + m_3)^2$. This discontinuity is given by Cutkosky's rule²⁵: One puts the two lines which cause the singularity on their mass shells, i.e., one replaces the two propagators by $-2\pi i \delta(p^2 - m^2)$. This corresponds to cutting the diagram as shown in Fig. 13. To integrate the δ functions, we introduce their arguments as new variables. The Jacobian is just the density $\nu = 2q/\sqrt{s}$ of intermediate states. The discontinuity is therefore the product of ν with the two simpler amplitudes in Fig. 13.

$$A^{(t)}(s+i\epsilon) - A^{(t)}(s-i\epsilon) = 2i\rho^{(t)}, \quad (13)$$

$$\rho^{(t)} = \nu A_0^{(r)} A_0^{(e)}. \quad (14)$$

$A_0^{(r)}$ is the s -wave projection of the resonance-production amplitude, and $A_0^{(e)}$ is, in general, the Feynman amplitude for the rescattering blob; in our case of a point interaction, it is $g/16\pi$.

We have arrived at the simple and important result that the discontinuity function (spectral function) of the triangle diagram is proportional to the amplitude of a simpler diagram, $A_0^{(r)}$, which by itself also contributes to the process.²⁷ The resonance production amplitude $A_0^{(r)}$ already contains all the kinematics of the triangle amplitude (except for the threshold at s_0 , which is introduced by the factor ν), and the discussion of triangle singularities reduces to the discussion of the simple pole term representing the resonance band on the Dalitz plot.

Let us assume for the moment that the triangle singularities lie on the second sheet. Then s_0 is the only

²⁷ This has already been noted by J. S. Ball, W. R. Frazer, and M. Nauenberg, Phys. Rev. **128**, 478 (1962).

singularity on the first sheet and we can write the dispersion integral

$$A_0^{(t)} = -\frac{1}{\pi} \int_{s_0}^{\infty} ds' \frac{\rho_0^{(t)}(s')}{s' - s}, \quad (15)$$

where the integration goes to ∞ , although the physical region only extends from $s_0 = (m_1 + m_3)^2$ to $s_1 = (W - m_2)^2$. This dispersion integral cannot be integrated explicitly using the commonly known functions of mathematical physics,²⁶ but it has the great advantage of exhibiting directly the complete sheet structure of $A^{(t)}$: The function on the first sheet, $A^I(s)$, is regular apart from s_0 . The function on the second sheet, A^{II} , is given by the downward analytic continuation of Eq. (14).

$$A^{II} - A^I = 2i\rho. \quad (16)$$

Therefore the singularities of A^{II} are the singularities of $2i\rho$:

$$\tilde{A}^{II} = 2i\tilde{\rho}. \quad (17)$$

Let us now check whether the position of the triangle singularities in the dispersion representation agrees with the prescription of Coleman and Norton. We have seen (Fig. 10) that for W^2 not far above threshold s_a is above and s_b below the real axis. The tentative dispersion integral implies that the triangle singularities are at the same place in the second sheet. This means that s_b , but not s_a , is on the physical boundary of $A_0^{(t)}$, as required by the theorem of Coleman and Norton. The dispersion integral is therefore correct.

As we increase W^2 , s_b moves around s_0 and gets above the real axis. It will then be near the wrong boundary of the physical sheet and therefore far away from the physical region.²⁸

We now complete the proof of the fundamental equation (12): The singularities of the triangle amplitude $A^{(t)}$ on the physical boundary are given by the singularities of the resonance-production amplitude $A^{(r)}$ below the axis (more exactly, below the contour of integration) as shown by Eq. (17). At s_b we have

$$\tilde{A}^{(t)} = 2i\tilde{\rho} = 2i\nu\tilde{A}_0^{(r)} A_0^{(e)} = (S_0 - 1)\tilde{A}_0^{(r)}, \quad (18)$$

which gives Eq. (12) immediately.

Let us now derive the fundamental equation in the framework of dispersion theory. We assume that the primary production is dominated by the resonance-production graph of Fig. 11(b) and that after the pri-

²⁸ As we increase W^2 still more, the singularity s_a of the spectral function crosses the real axis above s_0 and comes to lie below the axis. We can handle this in two ways. Either we let the singularity push down the contour in the dispersion integral, or we keep the path along the real axis and get an extra term. But in that case, the dispersion integral represents a function with the singularity s_a on the second sheet below the real axis, while $A^{(t)}$ has the singularity s_a on the first sheet below the real axis. The new term (which arose when we deformed the path of integration back to the real axis) will have the same structure on both sheets and it will cancel the singularity s_a of the dispersion integral on the second sheet and add the same singularity on the first sheet.

mary production only particles m_1 and m_3 interact, while m_2 escapes. (One should add the amplitude for the case where m_1 and m_2 interact, while m_3 escapes. For brevity, we shall omit this term.) We write down elastic unitarity in the (1, 3) system and we obtain for the discontinuity across the right-hand cut

$$\delta A_l/2i = \nu A_l A_l^{(el)*}. \tag{19}$$

The discontinuity of the Born term $A_l^{(r)}$ [Fig. 11(b)] approximates the discontinuity across the "left-hand" cut. However, note that our "left-hand" cut has moved to the right so that it connects the two triangle singularities s_a and s_b , and therefore it overlaps the right-hand cut (RHC). The Omnès-Muskhelishvili solution^{4,29} to this problem is

$$A_l = A_l^{(r)} + \frac{1}{\pi} \frac{1}{D_l^{(el)}} \int_{\text{RHC}} \frac{ds'}{s' - s} \nu A_l^{(r)} N_l^{(el)} + \frac{C}{D_l^{(el)}}, \tag{20}$$

and its three terms correspond to the three diagrams shown in Fig. 14. The singular part of Eq. (20) near s_b is

$$\tilde{A}_l = \tilde{A}_l^{(r)} + 2i\nu A_l^{(el)} \tilde{A}_l^{(r)} = S_l^{(el)} \tilde{A}_l^{(r)}, \tag{21}$$

which is again the fundamental equation.

D. Kinematics and Analytic Structure of the Born Amplitude

In order to introduce notation,¹² fill in details for part C, and to prepare for part E, we now discuss the Born amplitude $A_0^{(r)}$. For simplicity of notation, we treat the case where the two particles in the s channel have equal mass. We work in the rest frame of s [see Fig. 11(b)], \mathbf{p} is the momentum of W and m_2 , while $\pm \mathbf{q}$ are the momenta of m_1 and m_3 . The resonance production amplitude $A^{(r)}$ is

$$A^{(r)} = 1/(M_1^2 - t), \tag{22}$$

where the two coupling constants, which are common to all our amplitudes, are left out. In terms of the new variables s and $z_s = \cos(\mathbf{p}\mathbf{q})$, we have

$$2t = \sum_{i=1}^4 m_i^2 - s + 4pqz, \tag{23}$$

where m_i stands for the four external lines of Fig. 11(b). Introducing the abbreviations

$$\alpha \equiv s + 2M_1^2 - \sum_{i=1}^4 m_i^2, \tag{24}$$

$$r \equiv 4pq,$$

we get for the s -wave projection of $A^{(r)}$:

$$A_0^{(r)} = -\ln \frac{\alpha + r}{\alpha - r}, \tag{25}$$

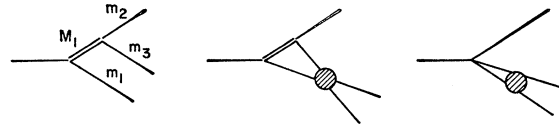


FIG. 14. Graphs which correspond to the Omnès-Muskhelishvili solution. The first graph represents the input (Born term), the other two arise from unitarity in the (1,3) channel.

where $r(s)$ is the phase-space factor of the three-body final state for a fixed s , i.e., it is the width of the Dalitz plot for that s value:

$$r = 4pq = t(s, z = +1) - t(s, z = -1), \tag{26}$$

$$2p = \left(\frac{(s_1 - s)(s_2 - s)}{s} \right)^{1/2}, \quad 2q = (s - s_0)^{1/2}, \tag{27}$$

$$s_0 = (m_1 + m_3)^2, \quad s_1 = (W - m_2)^2, \quad s_2 = (W + m_2)^2. \tag{28}$$

We now discuss the analytic structure of $A_0^{(r)}$ in the s plane. α is linear and therefore regular in s , while r has square-root branch points whenever it is zero or infinite. This happens at the thresholds s_0, s_1, s_2 , and at $s=0$. If we are on the main branch of the logarithm, we have

$$\frac{1}{r} \ln \frac{\alpha + r}{\alpha - r} = \text{even function of } r, \tag{29}$$

and r^2 in turn has no singularities at the thresholds. Therefore, the partial-wave amplitude $A_0^{(r)}$ is regular (in the first sheet) at all thresholds $(m_a \pm m_b)^2$ of the initial and final states. At $s=0$, r goes to infinity like a square root, the argument of the logarithm is -1 , and the imaginary part of the logarithm together with $1/r$ contributes a square-root branch point. On the other hand, the real part of the logarithm together with $1/r$ is regular again. For $\rho \equiv (g/16\pi)\nu A_0^{(r)}$, the situation is just the opposite: The imaginary part of the logarithm gives a regular contribution to ρ , while the real part contributes the branch point.

The leading singularities of $A_0^{(r)}$ arise when $(\alpha+r)$ or $(\alpha-r)$ vanishes. For real s , the vanishing of $(\alpha+r)$ or $(\alpha-r)$ means that the resonance band intersects the boundary of the Dalitz-Mandelstam plot for that value of s . This happens at most at two real points and the energies are the Peierls energies. For complex s , the Mandelstam-Dalitz plot is not useful. But we see from (24) and (27) that $s(\alpha+r) \cdot (\alpha-r)$ is a quadratic function in s , which does not vanish at $s=0$, and therefore $(\alpha+r)(\alpha-r)=0$ has exactly two solutions which must be the two Peierls energies, s_a and s_b .

Although $A_0^{(r)}$ looks quite complicated, if we insert the expressions for α and r , its analytic properties are very simple: On the physical sheet it has two logarithmic branch points at s_a and s_b , but it is regular everywhere else except at $s=0$ and at infinity, where it behaves like $(\ln s)/s$. On the other sheets (with respect to s_a and s_b) it has all threshold singularities.

²⁹ N. I. Muskhelishvili, *Singular Integral Equations* (P. Noordhoff, Ltd., Groningen, The Netherlands, 1953); R. Omnès, *Nuovo Cimento* **8**, 316 (1958); see also Ref. 4.

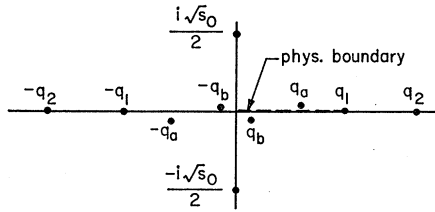


FIG. 15. Singularities of ρ and the points q_1 and q_2 .

E. An Explicit Expression for the Triangle Amplitude

Up to now, we have discussed the singular part of the triangle amplitude. Now we want to find a convenient expression for the entire amplitude, which is needed for comparison with experiment (e.g., the observation of the rescattering band in Ref. 19).

The triangle amplitude can be integrated²⁶ in terms of Spence functions. However, they are not tabulated, and so this means replacing one integral representation (the dispersion integral) by others (the ones for the Spence functions).

To take the dispersion integral, Eq. (15), directly to the computer¹² is not economical because the integrand is singular at $s'=s$, if we take s in the physical region. Moreover, the spectral function is singular at s_a and s_b , while the integral is singular only at s_b . This means that the peak at s_a must disappear in the process of numerical integration by means of an exact cancellation between contributions from the principle value of the integral and from the spectral function. We want to find a new representation, where these two unpleasant features are eliminated, and a discussion in the physical region becomes easy.

Cauchy integrals can be integrated easily in the following sense: We can write down immediately a function which has the proper discontinuity across the cut. However, this function will usually have unwanted singularities in the first sheet, which must be subtracted. This subtraction is nontrivial and leads to background terms in the form of dispersion integrals along distant cuts. These terms can be approximated easily.

In our case, we have a two-particle unitarity integral, and therefore the spectral function ρ behaves like a square root at threshold, i.e., it is an odd function of the momentum $q = \frac{1}{2}(s-s_0)^{1/2}$. Otherwise it is regular in s along the path of integration, since the triangle singularities have been removed from the real axis by the $i\epsilon$'s. The function with the proper discontinuity, $2i\rho$, across the cut from s_0 to ∞ is (because of the square-root behavior)

$$A_\alpha = i\rho, \tag{30}$$

where it is to be understood that the cuts of the ρ go from s_0 to the right and from $s=0$ to the left. A_α is the odd part of $A^{(t)}$ in the q plane. Let us now determine the even part.

Since $A^{(t)}$ is given by a dispersion integral, it is regular in the first energy sheet, which is the upper half

of the momentum plane. However, since $A_\alpha = i\rho$ is odd in q , it has logarithmic singularities at $\pm q_a$ and $\pm q_b$ and square-root singularities at $q = \pm (-s_0)^{1/2}/2$ corresponding to $s=0$ (Fig. 15). We now like to subtract all those singularities which are in the upper half plane (of Fig. 15) without introducing new singularities (at the points s_1 and s_2). This is, of course, impossible since it would mean an explicit integration of the amplitude. What we can do, however, is to subtract the triangle singularities in the first sheet and not yet bother with the singularity at $s=0$. This means that we subtract a function A_β which

- (i) has the same triangle singularities as A_α in the upper half plane, i.e., at $+q_a = (s_a - s_0)^{1/2}/2$ and at $-q_b = -(s_b - s_0)^{1/2}/2$ (see Fig. 15);
- (ii) is regular at threshold, i.e., even in q ;
- (iii) is regular everywhere else, in particular at s_1 and s_2 ; but we do not require that it also (iv) subtract the singularity at $q = +\frac{1}{2}i\sqrt{s_0}$, which corresponds to $s=0$ in the first sheet.

The Ansatz

$$A_\beta = \frac{i}{(s_1 - s)^{1/2}} \frac{i}{(s_2 - s)^{1/2}} \ln \frac{1+g}{1-g}, \tag{31}$$

with g meromorphic and $\neq 1$ except for the following prescriptions:

- (i) at $s = s_a$: $g = +1$, at $s = s_b$: $g = -1$,
- (ii) at $s = s_0$: $g = \text{even in } q$,
- (iii) at $s = s_1$: $g = (s - s_1)^{1/2} \times (\text{regular function})$, at $s = s_2$: $g = (s - s)^{1/2} \times (\text{regular function})$; determines A_β uniquely:

$$A_\beta = \frac{g}{16\pi \bar{p}} \frac{i}{\bar{p}} \ln \frac{(s - s_b)(\bar{p}_a + \bar{p}_b) + (s_a - s_b)(\bar{p} - \bar{p}_b)}{(s - s_a)(\bar{p}_a + \bar{p}_b) - (s_a - s_b)(\bar{p} - \bar{p}_a)}, \tag{32}$$

$$\bar{p} = (s_1 - s)^{1/2}(s_2 - s)^{1/2}, \quad \bar{p}_a = \bar{p}(s_a). \tag{33}$$

A_β subtracts most of the unwanted singularities of A_α in the first sheet. It remains to subtract the unwanted left-hand cut of A_α , which starts at $s=0$.

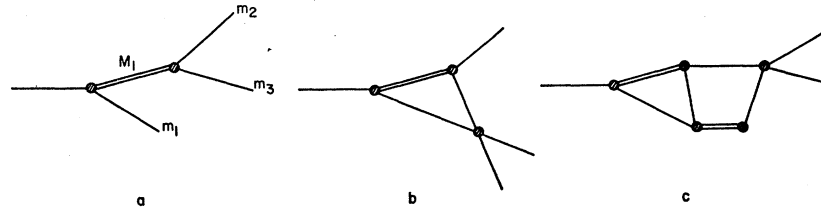
$$\delta A_\alpha / 2i = \text{Re} \rho \quad (-\infty \leq s \leq 0). \tag{34}$$

Note that ρ is essentially $\ln[(\alpha+r)/(\alpha-r)]$ and that the argument of the logarithm is real and negative to the left of $s=0$. This discontinuity cannot be subtracted by means of a function in closed form. Therefore we subtract it in the form of the dispersion integral A_γ :

$$A_\gamma = \frac{1}{\pi} \int_{-\infty}^0 ds' \frac{\text{Re} \rho(s')}{s' - s}. \tag{35}$$

This looks very much like the original expression for $A^{(t)}$ in Eq. (15). The important improvement is that A_γ is a dispersion integral over the distant interval

FIG. 16. Graphs for final-state interactions: (a) resonance production graph, its interference terms are discussed in Sec. III; (b) triangle graph, discussed in Sec. II; (c) higher order rescattering correction, does not lead to singularities on the physical boundary.



$s = (-\infty, 0)$, and its spectral function is finite, real, and positive, with one maximum between the two end-point zeros. In the physical region, A_γ contributes a real, small, and monotonically decreasing background which is easily evaluated numerically by hand. The full triangle amplitude $A^{(t)}$ is $A_\alpha - A_\beta - A_\gamma$. This has to be contrasted with the numerical integration of the full amplitude by Aitchison¹² and by Chang and Tuan,¹⁶ and with the proposal of Aitchison and Kacsner³⁰ to take the explicit expression for the nonrelativistic triangle amplitude and to simply guess what the relativistic generalization could be.

III. INTERFERENCE OF RESONANCE BANDS

After having seen that triangle singularities do not produce peaks, we now look at an entirely different mechanism, which also deals with final-state interactions: production of peaks by interference of overlapping resonance bands. We shall get a negative result again.

In this article we search for peaks produced by final-state interactions and assume that the singularities on the physical boundary will be the same in a theory of strong interactions as in perturbation theory. We discuss all graphs which lead to singularities close to the physical boundary, and which therefore correspond to classical processes in space-time (theorem of Coleman and Norton).⁵ There are only two classes of such graphs, the resonance production graphs [Fig. 16(a)], which will be discussed in this section, and the rescattering (or triangle) graphs [Fig. 16(b)], which have been discussed in Sec. II. The higher-order rescattering corrections [Fig. 16(c)] cannot be interpreted as classical processes. (For comments about an infinite sum of such diagrams, see the end of part IIB.) One resonance graph by itself leads to no surprising effects: It produces the resonance band on the Dalitz plot and a woolly cusp threshold in the total rate. However, it has been suggested that the interference of two (or more) bands gives interesting peaks. These peaks are conveniently discussed in terms of the kinematic relation

$$s+t+u = W^2 + \sum_{i=1}^3 m_i^2. \quad (36)$$

We shall explain first why one might expect interference effects to produce peaks:

(a) *Overlap of three-resonance bands at one point.* When a resonance exists in all three pairs (at s_R, t_R, u_R , respectively), formula (36) suggests a three-body peak for that total energy W_P^2 , which allows all three pairs to resonate simultaneously^{4,17}:

$$W_P^2 = s_R + t_R + u_R - \sum_{i=1}^3 m_i^2. \quad (37)$$

We demonstrate this situation on the Dalitz plot using a simple and often used, but misleading, approximation which consists of replacing the Breit-Wigner resonance bands by homogeneous bands of the width Γ and the constant amplitude $iM\Gamma$. Outside the bands, the amplitude is zero.

All three pairs resonating simultaneously means that all three bands overlap in one region and produce there a density of events 9 times higher than one resonance band by itself. This tremendous cluster of events on the Dalitz plot, which only appears at the total energy W_P^2 , is supposed to generate a peak in the total number of events on the Dalitz plot as a function of W^2 .

(b) *Interference of two-resonance bands producing a peak in the third pair.* If a resonance exists in only two of the three pairs, and the total energy is fixed at W_R^2 by nature (decay of a resonance, weak decay) or by the experiment (production process at fixed beam energy, $p\bar{p}$ annihilation at rest), then one might expect a peak for that energy s_P of the third pair which allows the two other pairs to resonate simultaneously^{4,31}:

$$s_P = W_R^2 - t_R - u_R + \sum m_i^2. \quad (38)$$

The situation on the Dalitz plot and the peak expected from our oversimplified model are shown in Fig. 17.

(c) *Threshold for overlapping resonances.* Assume again that a resonance exists in two of the pairs. When the overlap region moves into (out of) the Dalitz plot, a

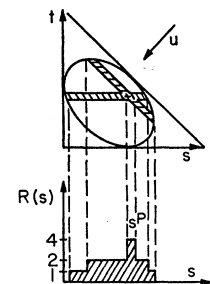


FIG. 17. Interference of two resonance bands producing a peak in the third pair. We shall show that such a peak does not occur in the limit of sharp resonances.

³⁰ I. J. R. Aitchison and C. Kacsner, Phys. Rev. **142**, 1104 (1966).

³¹ G. Goldhaber, *Lectures in Theoretical Physics* (University of Colorado Press, Boulder, Colorado, 1965), Vol. VII B, p. 343.

sharp increase (decrease) of the total rate as a function of s could be expected at W_b^2 (W_a^2).

$$W_{a,b}^2 = t_R + u_R + s_{\max, \min} - \sum_{i=1}^3 m_i^2. \quad (39)$$

Chang³² found that such a peak occurs for the overlap of ρ bands in the 3π system and suggested that it might explain the A_1 .

We note that the total energy $W_{a,b}^2$, at which these interference shoulders should appear, are exactly the Peierls energies and that s_{\min} is not the threshold value $s_0 = (m_1 + m_3)^2$, but rather the lowest s value for which overlap of the t and u bands inside the Dalitz plot is possible. This coincides with s_0 if the two resonances are the same.

Let us now see why interference effects cannot produce peaks of the type described above.

(a) *Overlap of three resonance bands at one point.*³³ A peak in the total rate could arise only from interference terms like

$$2 \operatorname{Re} \int \int [A_1(t)A_2^*(u)] dt du, \quad (40)$$

which do not even contain the information that a third resonance exists. The energy which allows all three pairs to resonate simultaneously cannot be a special point for this term. In other words, interference is a bilinear effect and is not affected by the overlap of *three* bands.

(b) *Interference of two resonance bands does not produce a peak in the third pair.* The contribution of the interference term to the invariant-mass distribution in the third pair is

$$2 \operatorname{Re} \int dt A_1(t)A_2^*(u), \quad (41)$$

where u depends on t and s . If the diameter of the overlap region is much smaller than the diameter of the Dalitz plot, then we can replace the limits of integration in Eq. (41), i.e., the boundaries of the Dalitz plot, by $\pm \infty$. We insert Breit-Wigner resonance amplitudes in Eq. (41),

$$2 \operatorname{Re} \int_{-\infty}^{+\infty} dt \frac{M_1 \Gamma_1}{t_1 - t - iM_1 \Gamma_1} \frac{M_2 \Gamma_2}{u_2 - u + iM_2 \Gamma_2}, \quad (42)$$

and see that the expression vanishes, because we can close and contract the contour in the upper half plane.

The exact result for a finite ratio of a Dalitz plot to overlap region shows how destructive interference be-

comes effective, as soon as the Dalitz plot becomes larger than the overlap region. The interference peak becomes smaller, until constructive and destructive interference cancel exactly for an infinitely large Dalitz plot or for infinitely sharp resonances.

(c) *Threshold for overlapping resonances.* In order to determine the effect of the overlap region moving into the Dalitz plot, its boundary is approximated by a straight line. This is a good approximation if the diameter of the Dalitz plot is much larger than the diameter of the overlap region.

The derivative of the total interference rate is proportional to the expression (41) with one important difference: There we integrated over a strip keeping s constant; now we integrate over a strip parallel to the boundary of the Dalitz plot. If $dt/du < 0$ along the interesting part of the boundary, then we get the same result as before, zero. But on the two arcs with $dt/du > 0$ the expression does not vanish. This is the same set of kinematical conditions as the ones under which the generalized Peierls singularity is near the physical boundary and not on the other sheet. We note that interference between two identical resonances ($M_1 = M_2$, $m_1 = m_2$), so-called symmetrization,³⁴ corresponds to the elastic Peierls case and produces no shoulders in the total rate. On the other hand, if we consider interference between two different resonances, $M_1 \neq M_2$, an effect is possible, but we do not know the relative, constant coefficient between the two amplitudes, because we do not know the numerator functions (in the N/D expression).

We can understand cancellation of interference effects if we recall that in optics interference does not create or destroy energy, it merely redistributes it. Similarly here, the total number of events on an infinite Dalitz plot is not changed by interference effects.³⁵ These effects merely redistribute events. Or, in other words, constructive interference is necessarily accompanied by destructive interference in an area not far away. If this other area happens to be outside the Dalitz plot, then and only then will the interference term give an effect.

In case (b), we had cancellation after integrating over a strip. This shows that interference shifts events around in a very special way: s (see Fig. 17) remains unchanged.

We do not claim that there is no effect at all in the cases (b) and (c). Rather, we have shown that the expected effects are absent in first order in Γ/d , where d is the diameter of the Dalitz plot.

We have not discussed the case of more than three particles in the final state,³⁶ where general statements become more difficult.

³² N. P. Chang, Phys. Rev. Letters **14**, 806 (1965).

³³ This argument has been communicated to A. H. Rosenfeld, who was kind enough to include it in his review in *Proceedings of the Oxford International Conference on Elementary Particles, Oxford, England, 1965* (Rutherford High Energy Laboratory, Chilton, Berkshire, England, 1966).

³⁴ C. Bouchiat and G. Flamand, Nuovo Cimento **23**, 13 (1962).

³⁵ The total number of interference events on an infinite Dalitz plot is logarithmically divergent. However, we have only used the derivative of the total interference rate, which is convergent.

³⁶ G. Goldhaber, in *Proceedings of the Second Coral Gables Conference on Symmetry Principles at High Energy*, edited by B. Kurşunoglu, A. Perlmutter, and I. Sakmar (W. H. Freeman and Company, San Francisco, California, 1966).

ACKNOWLEDGMENTS

I wish to express my gratitude to Professor F. E. Low for stimulating my interest in these questions and for valuable discussions, suggestions, and criticism. I should

also like to thank Professor S. C. Frautschi and Dr. F. Gilman for the critical reading of the manuscript. Finally, it is my pleasure to thank Professor L. Van Hove for the hospitality extended to me at CERN during the summer 1965, when this work was started.

Crossing Symmetry and Hadron Dynamics*

R. E. CUTKOSKY

Carnegie Institute of Technology, Pittsburgh, Pennsylvania

(Received 22 August 1966)

A method of carrying out bootstrap calculations is described in which analyticity properties enter indirectly. There are two main features: the use of a nonlinear Bethe-Salpeter equation which automatically maintains the symmetry properties of amplitudes, and the use of crossing symmetry in the construction of effective propagators. Two illustrative examples are considered. One is a simplified nonlinear equation for the familiar static model of baryon-meson interactions. The other is a model for interactions mediated by vector mesons.

I. INTRODUCTION

THE idea that the low-energy dynamics of hadrons is primarily governed by crossing symmetry is based on pioneering work by Chew, Low, and Mandelstam (CLM).^{1,2} In applying this principle, they developed an approximation scheme based on analyticity properties of the S matrix, practical exploitation of which requires a drastic truncation of the number of channels which are considered explicitly ("elastic unitarity," or various refinements). Since fluctuation in the number of particles is also an intrinsic feature of quantum field theory, it is not surprising that difficulties often appear when this feature is artificially suppressed.^{3,4} For this reason, there is interest in finding ways to implement the CLM principle which do not involve the CLM approximation. It is natural to consider, for this purpose, more old-fashioned methods of field theory—so called "off-mass-shell" techniques—which, by incorporating more detailed information about the variation of fields at nearby space-time points, automatically take better account of fluctuations in the number of quanta.⁵

The CLM principle involves the crossing symmetry of four-line diagrams; the effective potential acting between two particles is associated with exchange of

particles which arise as bound or resonant states in crossed channels, thereby giving rise to the cooperative features of hadron dynamics. Another aspect of crossing symmetry appears in three-line diagrams (which may also be considered as subsections of more complicated processes): The value of the vertex part must not depend on whether a given particle is outgoing or incoming. While this "vertex symmetry" does not directly influence the cooperative phenomena, it must be intrinsic to any valid calculational scheme. It is obvious that vertex symmetry is not compatible with any scheme in which the total number of particles which are considered to exist at any given time is arbitrarily limited.

It has been suggested that a calculational method with manifest vertex symmetry can be based on the Bethe-Salpeter (B-S) equation.⁶ So far, this method has been used only in a rather simplified approximation,^{7,8} and there may be some doubts as to how the method could be extended to higher orders of approximation. The purpose of this paper is to discuss such an extension, but for the sake of readability, we shall concentrate on the next order of approximation. The main problem concerning still higher orders of approximation appears to be how to decide which of several possible routes it would be most expeditious to follow.

The assumptions on which the procedure rests are as follows: We assume that some underlying local field theory exists and has the analyticity properties suggested by the regularized perturbation expansion.

* Supported, in part, by the U. S. Atomic Energy Commission.

¹ G. F. Chew and F. E. Low, *Phys. Rev.* **101**, 1570 (1956).

² S. Mandelstam, *Phys. Rev.* **112**, 1344 (1958). G. F. Chew and S. Mandelstam, *ibid.* **119**, 476 (1960).

³ R. F. Sawyer, *Phys. Rev.* **142**, 991 (1966).

⁴ R. E. Cutkosky, in *Particle Symmetries* (1965 Brandeis University Summer Institute in Theoretical Physics, Vol. II), edited by M. Chretien and S. Deser, [Gordon and Breach, Science Publishers, Inc., New York, (1966)], p. 97.

⁵ The usefulness of the field idea in self-consistent models has been emphasized by J. Schwinger, *Phys. Today* **19**, No. 6, 27 (1966).

⁶ R. E. Cutkosky and M. Leon, *Phys. Rev.* **135**, B1445 (1964).

⁷ R. E. Cutkosky and M. Leon, *Phys. Rev.* **138**, B667 (1965).

⁸ K. Y. Lin and R. E. Cutkosky, *Phys. Rev.* **140**, B205 (1965); K. Y. Lin, Carnegie Institute of Technology dissertation, 1966 (unpublished).